

Mapping of Flood Risk Areas and Prevention Measures: A Case Study of Foum Elkhanga Watershed

Faiza Balla¹, Chems Eddine Bouhadeb²

¹Departement hydraulic, university of ziane achour, djelfa, 1700, algeria

²Water Resources and Sustainable Development Laboratory, Badji Mokhtar – Annaba University, P.O. Box 12, 23000, Annaba, Algeria.

*email: faiza.balla@univ-djelfa.dz

ARTICLE INFO

ABSTRACT

Received: 25 Jun 2025

Revised: 21 Sep 2025

Accepted: 28 Nov 2025

Introduction: Floods are major natural disasters resulting from multiple environmental and anthropogenic factors. They cause considerable damage, affecting not only soil and agricultural production, but also infrastructure, material goods and, above all, the safety of local populations. South eastern Algeria, specifically the town of Sedrata, which encompasses the Foum Elkhanga watershed, is among the areas most vulnerable to this recurring phenomenon.

Objectives: The objective of this study is to produce a map of the potential flood risk in oued foum elkhanga watershed, using the MCDA-AHP model, as well as to validate the reliability of the results obtained.

Methods: Flood susceptibility mapping can be carried out using several approaches. However, one of the most effective methods is based on multi-criteria analysis (MCDA) combined with the analytical hierarchy process (AHP). In this context, the AHP method was used to assign a relative weight to each conditioning factor. These factors were then combined using an overlay weighting technique in geographical information systems (GIS).

Results: The results show that flood susceptibility can be classified into four levels Low risk, Moderate risk, High risk, and very High risk. In general, the majority of areas classified as high risk are located in the city of Sedrata, close to the Fum Elkhanga dam, while areas classified as low, moderate and very high risk are mainly located in mountainous areas. Validation of the model, carried out by comparing the map produced with flood events recorded between 2002 and 2024, reveals an area under the ROC curve average of 78.3%, indicating a high level of accuracy and confirming the validity of the susceptibility map obtained.

Conclusions: The analysis also highlights the relevance of the conditioning factors used. Nine variables proved to be decisive in the modelling: TWI, Elevation, Slope, Rainfall, LULC, NDVI, Distance from River, drainage density, and Soil type.

Keywords: Flood, Foum Elkhanga watershed, MCDA-AHP model.

INTRODUCTION

Natural disasters can be triggered either by strictly environmental processes or by human activities [1]. Natural hazards generally manifest themselves according to the dynamics specific to physical and ecological systems, and can be anticipated when their characteristics are well identified [2,3]. Conversely, man-made disasters often occur suddenly, resulting from inadequate resource management or low environmental awareness [4]. In addition, certain human activities can intensify or accelerate natural phenomena, leading to extreme events outside their usual periods [5].

Among these hazards, floods are among the most destructive. They cause human casualties, considerable material damage and lasting disruption to economic, social and urban dynamics [6,7]. Their sometimes-unpredictable nature they can even occur during the dry season poses a major challenge for scientific research and environmental management [8]. Globally, floods remain a major concern due to their serious impacts, including loss of life [9].

In urban contexts, several factors increase the risk of flooding, including: inadequate or failing drainage systems [10], rapid population growth, increasing surface impermeability due to urbanisation, inefficient waste management leading to the obstruction of drainage channels [11,12]. Indonesia is particularly vulnerable to flooding, as illustrated by the major events in Sintang in 2021 and Manado in 2014, which caused significant human and material damage [13,14]. In the Bandung Raya region, flooding is a recurring phenomenon, particularly in the districts of Baleendah and Dayeuhkolot, where significant flooding was recorded in 2020 [15].

Bandung Raya's vulnerability can be explained by several factors: high urban density, low vegetation cover, and sloping topography that encourages water to flow towards built-up areas [16]. The region comprising the city of Bandung, Cimahi, Bandung District, and West Bandung District is crossed by numerous watercourses converging towards the south, thereby increasing its exposure to flooding [17].

Flood risk mapping is based on the integration of multiple factors specific to the geographical context and spatial scale under study. Commonly used parameters include NDVI, land use, TWI, precipitation, slope, altitude, and distances to roads and watercourses [18,19,20]. The respective influence of these variables may vary depending on regional specificities and the quality of available data [21,22].

In this context, the use of GIS combined with multi-criteria approaches offers a robust method for spatial modelling and the production of susceptibility maps [23,24]. Among these methods, Multi-Criteria Decision Analysis (MCDA) based on the Analytic Hierarchy Process (AHP) is widely used to establish the weighting of criteria through pairwise comparisons [25,26]. AHP is notable for its flexibility and adaptability to various contexts, although some critics point to its subjective nature [27].

In this study, nine factors were selected to develop the Fum Elkhanga watershed flood susceptibility map: TWI, altitude, slope, precipitation, land use (LULC), NDVI, distance to rivers, and distance to roads. The MCDA-AHP model was applied and validated using flood events recorded between 2002 and 2022. This approach makes it possible to identify the most vulnerable areas in the Fum Elkhanga watershed, in order to produce a reliable susceptibility map based on weighted linear combination.

MATERIALS AND METHODS

STUDY AREA

The Oued Cherf/Sedrata watershed, identified by hydrological code (14.01) according to the National Agency for Hydrographic Basins, is located in north-eastern Algeria, upstream from the Foun El Khanga dam. It forms a border area between three wilayas: Souk Ahras, Guelma and Oum El Bouaghi, and comprises seven administrative districts. This basin, which belongs to the Seybouse hydrographic system, is triangular in shape and covers an area of approximately 1,767 km². It is bounded to the north by Djebel Tifféch, the Ras El Alia massif and Djebel Zouabi; to the south by Djebel Ezzorg, Koudiat Edabdaba and Djebel Lahmar; to the east by the Djebel Kebarit, Djebel Teraguelet and Djebel Ain Zitouna massifs; and to the west by Djebel Sidi Réghiss and Chebkat Sellaoua (Figure 1).

Research Article

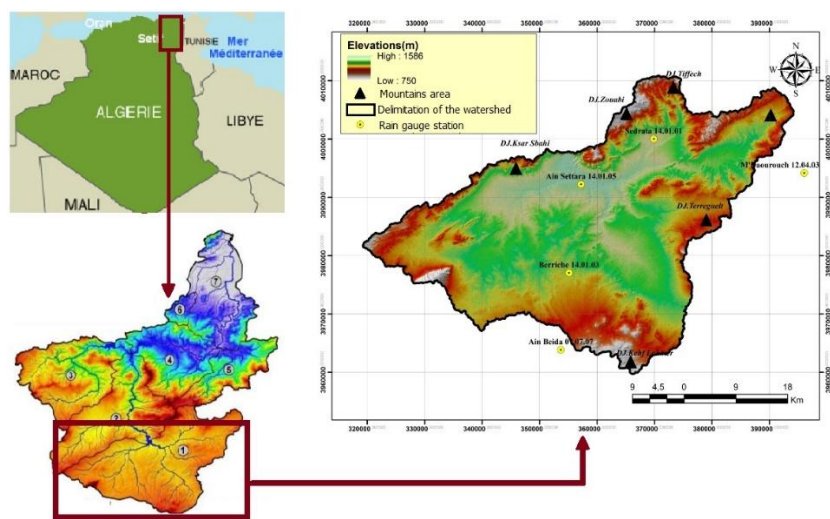


Figure 1: Geographical location of the study area

The south-eastern sector is continuous with the high plains of the Haute-Seybouse and the upper Medjerda valley, where the watersheds between the Seybouse, Cherf and Medjerda basins are located, near Ras El Alia, the birthplace of the Krab and Tiffech wadis, both tributaries of the Cherf. To the south, the high plains of the Cherf connect with those of the salt flats of Guéllif, Tarf and Ank Djemel, forming a gently undulating landscape punctuated by small isolated massifs such as Djebel Sidi Réghiss (1,623 m), whose northern slope extends into the Seybouse hydrographic domain (Figure 2).

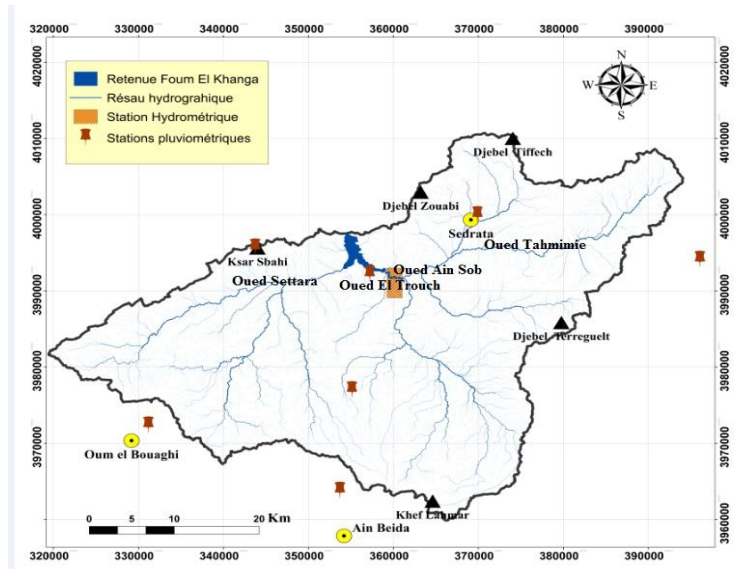


Figure 2: Hydrographic situation of the study area

The relief, with its variations in altitude and morphology, strongly influences the hydrological processes of the basin, particularly the distribution of precipitation, surface runoff and runoff velocity, making topography a determining factor in regional hydrological dynamics.

The streams located in the south-east of the catchment area converge in the Sedrata region to form the El Hamimine wadi. Next comes the Aïn Snob wadi, which rises in Chott El Magène and Djebel Teraguelet, at the furthest points from the large Seybouse basin, and then forms the Trouch wadi. The streams located to the south-west converge to form the Settara wadi, composed of the Aïn Babouche wadi and the El Mebdoua wadi. These tributaries are fed by

small streams descending from Djebel Sidi Reghiss, north of Oum El Bouaghi, as well as from the eastern flank of the Chebkat Sellaoua mountain range.

The junction of the two wadis, the Trouch and the Settara, gives rise to the Cherf, which flows at the foot of Djebel Zouabi before emptying into the Foum El Khangua dam basin.

DATA AND METHODOLOGICAL APPROACHES

The data used in this research requires a variety of data collected from different credible and valid sources, which are then processed in a GIS. Based on the description of the literature review presented in the introduction, the data used for flood vulnerability processing can be found in Table 1.

Eight types of data are used as flood vulnerability factors, and these data were also selected to avoid excessive complexity in processing data at the regional level, covering four major cities. The eight data sets are: (1) TWI; (2) Elevation; (3) Slopes; (4) Rainfall (Precipitation); (5) LULC; (6) NDVI; (7) Distance from rivers; (8) drainage density; and (9) Soil type (figure 3). The ninth data set is used to validate the flood susceptibility map, based on flood data from 2001 to 2024.

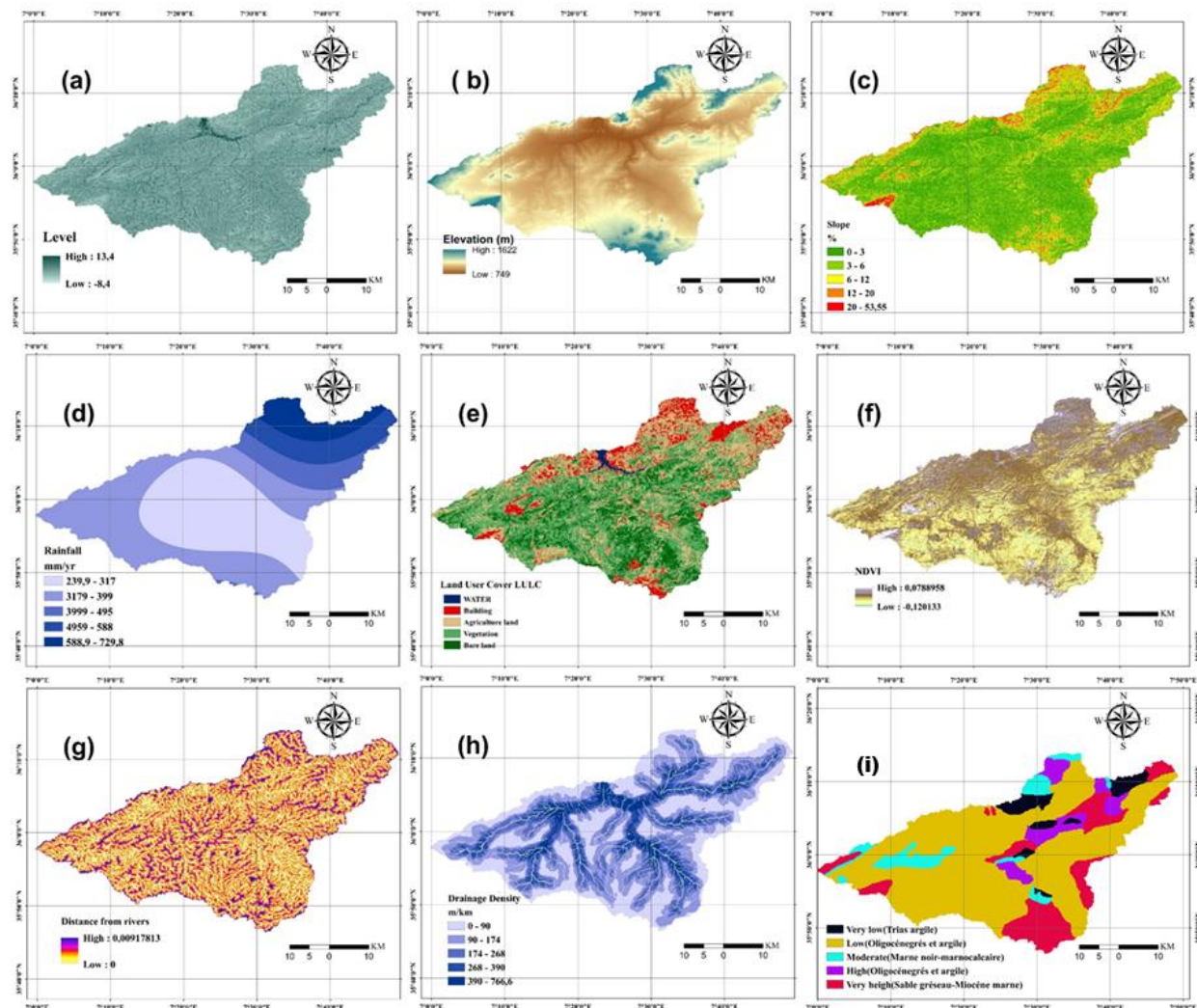


Figure 3: Characteristic distributions of risk factors.

In this study, GIS was used to collect and analyse all flood vulnerability factors in the local GIS database. All operations involving the conditioning and reclassification of factor maps, weighted linear combinations (WLC), and

validation of the flood susceptibility map for the Fumelkhanga watershed were performed using GIS. All functions used in the GIS analysis are considered solely in their spatial form.

Table 1: Sources of data used in this study

No	Data type	GIS data type		Scale or resolution	Source of data
		Spatial database	Derived map		
1	TWI	GRID	Slope Gradient (°)	30 m	Digital Elevation Model (DEM)
2	Elevation	GRID	Elevation (m)		Digital Elevation Model (DEM)
3	Slope	GRID	Topographic wetness index		Digital Elevation Model (DEM)
4	Rainfall	GRID	-		National Agency for Water Resources
5	LULC	ARC/INFO GRID	Land use	10 m	ESRI Land Cover (2024)
6	NDVI	ARC/INFO GRID	NDVI	30 m	Landsat 8 OLI/TIRS+ Images
7	Distance from River	GRID	Distance from River	30 m	Digital Elevation Model (DEM)
8	Distance from Road	GRID	Distance from Road	30 m	Digital Elevation Model (DEM)
9	Soil type	GRID	Soil type		National Institute of Cartography
10	Flood Inventory	Point and Polygon	-	-	Disaster Information Data of Algeria

Figure 4 shows the methodology adopted in this study.

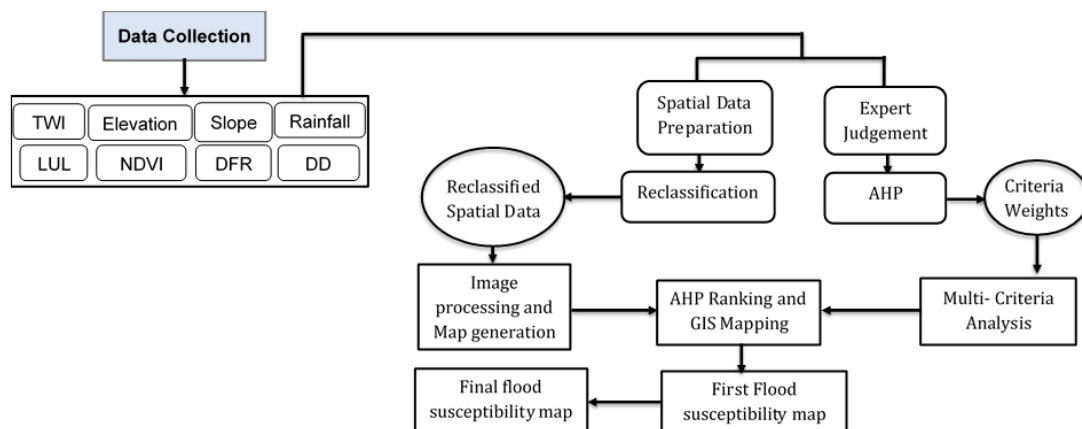


Figure 4: The methodology framework

MODEL VALIDATION

The validation or expert in this research uses the AHP method, performed using Microsoft Excel software by carrying out quantitative planning, in which the preference scale is used to make decisions from a series of available alternatives [28]. The pairwise comparison matrix (PCM) is used in AHP to establish a ranking of the available parameters, where this PCM allows a weighting factor to be constructed for each criterion given by each individual, applying the ranking scale [29].

The weighting scale for conditioning factors can be chosen on a scale of 1 to 9, where scale 1 indicates that the importance of the two conditioning factors is equal, and scale 9 indicates a very high importance for one of the selected conditioning factors. The random average values of the consistency index (CI) generated by the PCM (RI) will vary depending on the number of conditioning factors used, with different sequences of matrices presented. The consistency ratio (CR) shows the data validation results that will be used later in a quantitative manner, according to a mathematical equation presented in Eqs. 1 and 2.

$$CR = \frac{CI}{RI}$$

1

$$CI = \frac{(\gamma_{max-n})}{n - 1}$$

2

The RI data were obtained from the results of the randomly selected PCM, which was constructed from the pairwise comparison table in a random and inconsistent manner (Swain et al., 2020). To validate the weights of the conditioning factors used, the CR value must be <0.1 ; if the CR value is >0.1 , then the weighting matrix established by the experts must be recalculated. Any form of weighting aimed at normalising the PCM value is carried out using different techniques or approaches, depending on the experts' opinions [30].

Then, after obtaining the weights from the expert assessment, the aggregation method is used to multiply each conditioning factor in the form of a map in GIS, based on the acquisition of the weights of the factors according to Eq. 3.

$$FS = \sum w_i x_i$$

Were,

FS: Flood susceptibility; w_i : Weight of factor; i and x : Classes of flood susceptibility for each factor i

The spatial map is created from data obtained from the sources presented in Table 1. Next, all data are harmonised at the unit level if they differ, in order to avoid any imbalance in the data. All spatial data are classified into five categories according to their unit.

After classification, the data is weighted using an appropriate weighting, where the values of the conditioning factors are adjusted according to the results obtained with the AHP method during the expert judgement stage. The cartographic results obtained are then validated. It should be noted that if the data are not valid, they are repeated and verified again from the beginning, then validated using the Receiver Operating Characteristic (ROC) method, which calculates an Area Under Curve (AUC) value. The AUC value is then multiplied by 100% to obtain a percentage. This AUC value is then categorised according to the interpretation level, with a value greater than 0.7 being considered valid [31].

RESULTS AND DISCUSSION

RESULTS

This study presents nine types of data from a map of conditioning factors that may influence flood vulnerability; the data used are presented in Table 1. Some images need to be converted because they have different data units than those desired by the researcher [31].

Once the data has been correctly obtained and its quality and resolution are sufficiently usable or suited to the needs, the researcher then reclassifies it according to predefined values. The purpose of this reclassification is to specify the classes that will appear later, but the final classes depend on the availability and weight of the data. The results of the reclassification based on the class or value of each map are presented in Table 2.

Once the weightings have been carried out by five validations, only one condition must be ensured: that the CR value by expert judgement does not exceed 0.1. The weighting results of each expert are then calculated. With the application of the AHP method to determine the weighting criteria, the values are normalised from the principal eigenvector, obtained by comparing the values of each row to obtain the total weight of all flood susceptibility criteria for Foum Elkhanga. Show in figure 5 and figure 7 the Matrix of Classes between conditioning factors, and estimated ratings. The result is a sigma max value of 8081 and a CR value of 0.8, which shows that the weighting data validation is correct, as $CR (14.4) < 20$. The validity of the results predictions was tested using the receiver operating characteristic (ROC) model and its area under the curve (AUC) (figure 6).

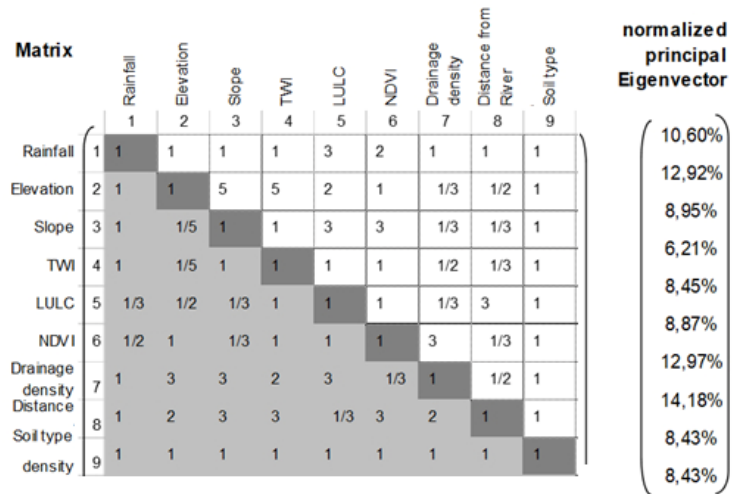


Figure 5: Matrix of Classes between conditioning factors, and estimated ratings %

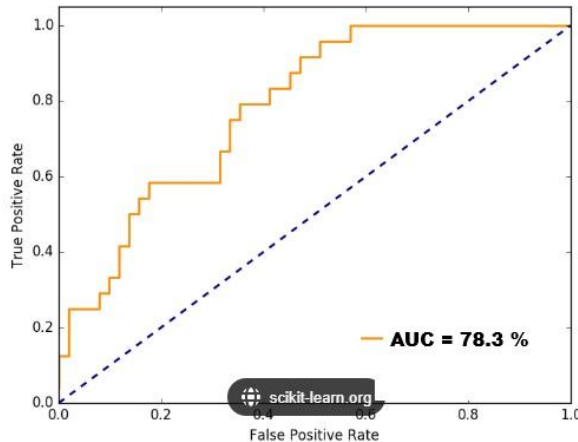


Figure 6: Model validation results by Random Forest

Finally, the weighting results for each conditioning factor are applied in GIS using a weighted overlay to create a flood susceptibility map for Foum Elkhanga, with the results of the flood susceptibility map for the region.

Table 2: Classes of conditioning factors, and estimated ratings for reclassify

Flood causative criterion	unit	class	Susceptibility class ranges and ratings	Susceptibility class ratings	Weight (%)
NDVI	ND	-0,12-0,04	Very Low	1	10,6
		-0,04-0,02	Low	2	
		-0,02-0,015	Moderate	3	
		-0,015-0,003	high	4	
		-0,003-0,08	very high	5	
Distance from river	m	0-0,0008	Very Low	1	14,4
		0,0008-0,003	Low	2	
		0,003-0,005	Moderate	3	
		0,005-0,006	high	4	
		0,006-0,01	very high	5	
Draiage density	m/km	0-90	Very Low	1	8,43
		90-174	Low	2	
		174-268	Moderate	3	
		268-390	high	4	
		390-767	very high	5	

Soil type	Level	Triassic clay Quaternary marl Black marl – marl-limestone Oligocene sandstone and clay Sandy sandstone – Miocene marl	Very Low Low Moderate high very high	1 2 3 4 5	7,82
Elevation	m	749-836 836-987 902-987 987-1138 1138-1622	Very Low Low Moderate high very high	1 2 3 4 5	12,92
Slope	%	0-3 3-6 6-12 12-20 20-50	Very Low Low Moderate high very high	1 2 3 4 5	8,95
TWI	Level	-8,4-4,8 -4,8-3,04 -3,04-0,57 -0,57-2,93 2,94-13,4	Very Low Low Moderate high very high	1 2 3 4 5	6,21
LULC	Level	Water Agriculture land 2 Building 3 Bare land 4 Vegetation	Very Low Low Moderate high very high	1 2 3 4 5	8,45
Rainfall	Level	239,9-317 317-399 399-495 495-588 588-729,8	Very Low Low Moderate high very high	1 2 3 4 5	10,6

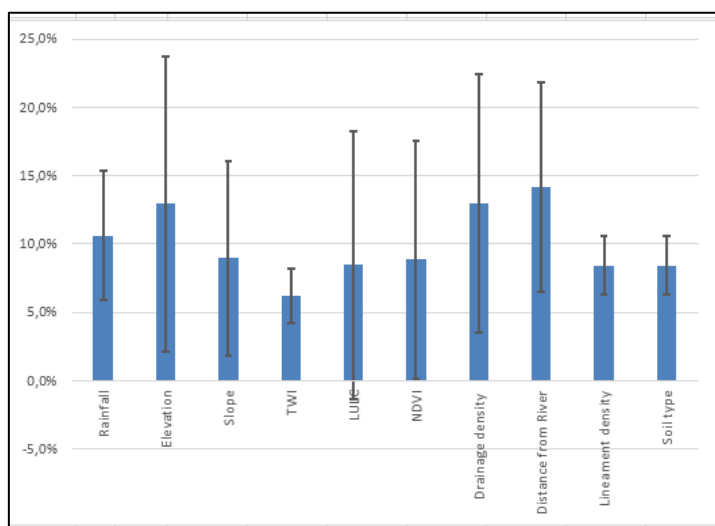


Figure 7: Classes of conditioning factors, and estimated ratings %

DISCUSSION

The spatial distribution of flood risk at the basin scale results from combining the various thematic layers of the model factors discussed above. The final results show that this hazard is prevalent in the flood risk area located in the centre of the basin, exactly in the main thalwegs. These flood risk have been grouped into five classes: very low, low, moderate, high and very high, according to the vulnerability rate (figure 8).

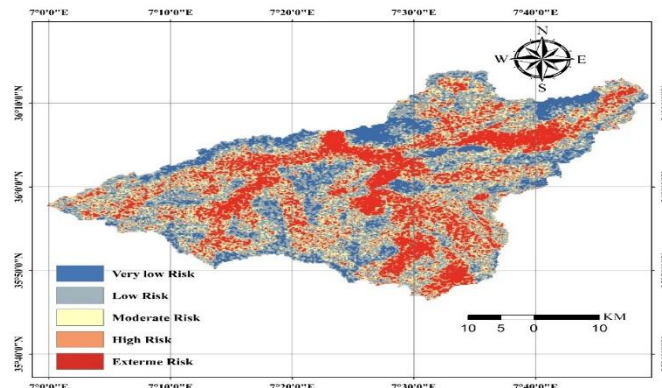


Figure 8: flood susceptibility map

Approximately 30% of the Oued Cherf watershed is exposed to a high risk of flooding. These areas are mainly located in sectors characterised by moderate to steep slopes and moderately dense to very sparse vegetation cover. They largely correspond to agricultural land located on relatively steep slopes, which increases vulnerability to flooding.

Areas with low risk of flooding are mainly found in the moderate parts of the watershed, where slopes are gentle or vegetation is dense. Conversely, high risk of flooding values are associated with fragile soils which can impact agricultural production—as well as rugged terrain with degraded vegetation. These conditions promote erosion and increase the risk of flooding. showing vulnerability classes in km² and % (table 3, figure 9)

Table 3: Flood Risk classes

CLASSE	Flood Risk	Area Km ²	Area%
1	Very low risk	315	18
2	low risk	484	27
3	Moderate risk	398	23
4	High risk	140	8
5	High risk	430	24

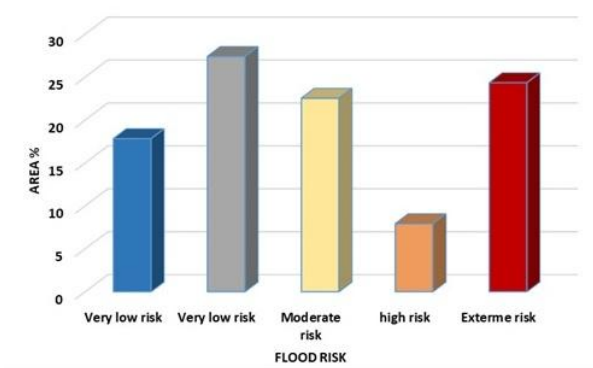


Figure 9: Flood Risk area in %

CONCLUSION

The study used the AHP–MCDA method with GIS software to map flood susceptibility in Foum Elkhanga watershed. Five risk levels were identified: very low, low, moderate, high and extreme. The centre of the Foum Elkhanga watershed (1,767 km²) and the Sedrata plain and town are mainly classified as high to very high risk, while the mountains and hills are dominated by moderate to low risk areas. The validation results (average AUC of 78.3%) confirm the

reliability of the map, which can be used as a tool by local authorities to prioritise areas at high or very high risk of flooding.

REFERENCES

- [1] Torani, S., Majd, P. M., Maroufi, S. S., Dowlati, M., & Sheikhi, R. A. (2019). L'importance de l'éducation sur les catastrophes et les situations d'urgence : un article de synthèse. *Journal of Education and Health Promotion*, 8(1), 85. https://doi.10.4103/jehp.jehp_262_18
- [2] Dysarz, T., Marcinkowski, P., Wicher-Dysarz, J., Piniewski, M., Mirosław-Świątek, D., & Kundzewicz, Z. W. (2025). Assessment of climate change impact on flood hazard zones. *Water Resources Management*, 39(2), 963-977. <https://doi.org/10.1007/s11269-024-04002-8>
- [3] Tabasi, N., Fereshtehpour, M., & Roghani, B. (2024). A Review on Flood Risk Conceptual Frameworks and Development of Hierarchical Structures for Assessment Criteria. *arXiv preprint arXiv:2409.08803*. <https://doi.org/10.1007/s43832-025-00193-2>
- [4] Fernandes, F., Malheiro, A., & Chaminé, H. I. (2023). Natural hazards and hydrological risks: climate change-water-sustainable society nexus. *SN Applied Sciences*, 5(1), 36. <https://doi.org/10.1007/s42452-022-05214-6>
- [5] Ullah, K., & Zhang, J. (2020). GIS-based flood hazard mapping using relative frequency ratio method: A case study of Panjkora River Basin, eastern Hindu Kush, Pakistan. *Plos one*, 15(3), e0229153. <https://doi.org/10.1371/journal.pone.0229153>
- [6] Ibrahim, M., Huo, A., Ullah, W., Ullah, S., Ahmad, A., & Zhong, F. (2024). Flood vulnerability assessment in the flood prone area of Khyber Pakhtunkhwa, Pakistan. *Frontiers in Environmental Science*, 12, 1303976. doi:10.3389/fenvs.2024.1303976
- [7] Moe, I. R., Kure, S., Farid, M., Udo, K., Kazama, S., & Koshimura, S. (2015). *Numerical simulation of flooding in Jakarta and evaluation of a counter measure to mitigate flood damage*. *Journal of Japan Society of Civil Engineers, Ser. G (Environmental Research)*, 71(5), I_29–I_35. https://doi.org/10.2208/jscejer.71.I_29
- [8] Mosavi, A., Ozturk, P., & Chau, K. W. (2018). Flood prediction using machine learning models: Literature review. *Water*, 10(11), 1536. <https://doi.org/10.3390/w10111536>
- [9] He, B., Huang, X., Ma, M., Chang, Q., Tu, Y., Li, Q., ... & Hong, Y. (2018). Analysis of flash flood disaster characteristics in China from 2011 to 2015. *Natural Hazards*, 90(1), 407-420. <https://doi.org/10.1007/s11069-017-3052-7>
- [10] Shi, W., Huang, S., Zhang, K., Liu, B., Liu, D., Huang, Q., Fang, W., Han, Z., & Chao, L. (2022). Quantifying the superimposed effects of drought-flood abrupt alternation stress on vegetation dynamics of the Wei River Basin in China. *Journal of Hydrology*, 612, 128105. <https://doi.org/10.1016/j.jhydrol.2022.128105>
- [11] Bamberg, S., Masson, T., Brewitt, K., & Nemetschek, N. (2017). Threat, coping and flood prevention—A meta-analysis. *Journal of Environmental Psychology*, 54, 116-126. <https://doi.org/10.1016/j.jenvp.2017.08.001>
- [12] Yusoff, I. M., Ramli, A., Alkasirah, N. A. M., & Nasir, N. M. (2018). Exploring the managing of flood disaster: A Malaysian perspective. *Geografia*, 14(3).
- [13] Putra, P. B., Auliyani, D., & Adi, R. N. (2022). Sintang Regency flood analysis of 2021. In *IOP Conference Series: Earth and Environmental Science*, Vol. 1109, No. 1, p. 012020. IOP Publishing. doi:10.1088/1755-1315/1109/1/012020
- [14] Langkai, J. E., & Pangkey, I. (2023). Evaluation of flood and landslide management program in Manado City. In *Unima International Conference on Social Sciences and Humanities (UNICSSH 2022)* (pp. 1676-1682). Atlantis Press.
- [15] Nurwulandari, F. S., & Rismana, G. A. (2021). Community resilience to face flood disaster in the Baleendah Village, Bandung Regency, Indonesia. In *IOP Conference Series: Earth and Environmental Science*, Vol. 737, No. 1, p. 012051. IOP Publishing.
- [16] Afriyanie, D., Julian, M. M., Riqqi, A., Akbar, R., Suroso, D. S., & Kustiwan, I. (2020). Re-framing urban green spaces planning for flood protection through socio-ecological resilience in Bandung City, Indonesia. *Cities*, 101, 102710.

[17] Putra, R. P., Agustina, R. D., Susanti, S., Chusni, M. M., & Novitasari, E. (2023). Flood Hazard Mapping in Bandung Regency Based on Multi-Criteria Decision Analysis (MCDA) with AHP Method. *Indonesian Review of Physics*, 6(2), 82-91. doi: 10.12928/irip.v6i2.10386.

[18] Hammami, S., Zouhri, L., Souissi, D., Souei, A., Zghibi, A., Marzougui, A., & Dlala, M. (2019). Application of the GIS based multi-criteria decision analysis and analytical hierarchy process (AHP) in the flood susceptibility mapping (Tunisia). *Arabian Journal of Geosciences*, 12(21), 653. <https://doi.org/10.1007/s12517-019-4754-9>

[19] Costache, R. (2019). Flash-flood Potential Index mapping using weights of evidence, decision Trees models and their novel hybrid integration. *Stochastic Environmental Research and Risk Assessment*, 33(7), 1375-1402. <https://doi.org/10.1007/s00477-019-01689-9>

[20] Rahmati, O., Darabi, H., Panahi, M., Kalantari, Z., Naghibi, S. A., Ferreira, C. S. S., Kornejady, A., Karimidastenaei, Z., Mohammadi, F., Stefanidis, S., Tien Bui, D., & Haghghi, A. T. (2020). Development of novel hybridized models for urban flood susceptibility mapping. *Scientific reports*, 10(1), 12937. <https://doi.org/10.1038/s41598-020-69703-7>

[21] Vojtek, M., Vojteková, J., Costache, R., Pham, Q. B., Lee, S., Arshad, A., ... & Anh, D. T. (2021). Comparison of multi-criteria-analytical hierarchy process and machine learning-boosted tree models for regional flood susceptibility mapping: a case study from Slovakia. *Geomatics, Natural Hazards and Risk*, 12(1), 1153-1180. <https://doi.org/10.1080/19475705.2021.1912835>

[22] Cabrera, Jonathan Salar, and Han Soo Lee. Flood risk assessment for Davao Oriental in the Philippines using geographic information system-based multi-criteria analysis and the maximum entropy model. *Journal of Flood Risk Management* 13.2 (2020): e12607. <https://doi.org/10.1111/jfr3.12607>

[23] Khadka, N., Chen, X., Nie, Y., Thakuri, S., Zheng, G., & Zhang, G. (2021). Evaluation of Glacial Lake Outburst Flood susceptibility using multi-criteria assessment framework in Mahalangur Himalaya. *Frontiers in Earth Science*, 8, 601288. doi: 10.3389/feart.2020.601288

[24] Wu, Y., Sun, J., Hu, B., Zhang, G., & Rousseau, A. N. (2023). Wetland-based solutions against extreme flood and severe drought: Efficiency evaluation of risk mitigation. *Climate risk management*, 40, 100505. <https://doi.org/10.1016/j.crm.2023.100505>

[25] Samanta, R. K., Bhunia, G. S., Shit, P. K., & Pourghasemi, H. R. (2018). Flood susceptibility mapping using geospatial frequency ratio technique: a case study of Subarnarekha River Basin, India. *Modeling Earth Systems and Environment*, 4(1), 395-408. <https://doi.org/10.1007/s40808-018-0427-z>

[26] Tang, Z., Zhang, H., Yi, S., & Xiao, Y. (2018). Assessment of flood susceptible areas using spatially explicit, probabilistic multi-criteria decision analysis. *Journal of Hydrology*, 558, 144-158. <https://doi.org/10.1016/j.jhydrol.2018.01.033>

[27] Cai, S., Fan, J., & Yang, W. (2021). Flooding risk assessment and analysis based on GIS and the TFN-AHP method: a case study of Chongqing, China. *Atmosphere*, 12(5), 623. <https://doi.org/10.3390/atmos12050623>

[28] Chourabi, Z., Khedher, F., Babay, A., & Cheikhrouhou, M. (2019). Multi-criteria decision making in workforce choice using AHP, WSM and WPM. *The Journal of The Textile Institute*, 110(7), 1092-1101. <https://doi.org/10.1080/00405000.2018.1541434>

[29] Swain, K. C., Singha, C., & Nayak, L. (2020). Flood susceptibility mapping through the GIS-AHP technique using the cloud. *ISPRS International Journal of Geo-Information*, 9(12), 720. <https://doi.org/10.3390/ijgi9120720>

[30] Choudhury, K. N., Yabar, H., & Mizunoya, T. (2022). GIS and remote sensing-based spatiotemporal analysis of cumulative flood risk over Bangladesh's national highways. *Asia-Pacific Journal of Regional Science*, 6(1), 335-364. <https://doi.org/10.1007/s41685-021-00216-5>

[31] Nachappa, T. G., Piralilou, S. T., Gholamnia, K., Ghorbanzadeh, O., Rahmati, O., & Blaschke, T. (2020). Flood susceptibility mapping with machine learning, multi-criteria decision analysis and ensemble using Dempster Shafer Theory. *Journal of hydrology*, 590, 125275. <https://doi.org/10.1016/j.jhydrol.2020.125275>

[32] Cabrera, J. S., & Lee, H. S. (2020). Flood risk assessment for Davao Oriental in the Philippines using geographic information system-based multi-criteria analysis and the maximum entropy model. *Journal of Flood Risk Management*, 13(2), e12607. <https://doi.org/10.1111/jfr3.12607>